Error Analysis of the Discrete Complex Image Method and Pole Extraction

Swee-Ann Teo, *Member, IEEE*, Siou-Teck Chew, *Member, IEEE*, and Mook-Seng Leong, *Senior Member, IEEE*

***Abstract*—Recently, Teo *et al.* proposed a discrete complex image method that is able to represent both the near and far fields of the Green's function accurately, using only a single approximate Green's function. In this paper, an error analysis of this method is presented. The error analysis shows an additional term, which represents the quasi-static image of the surface-wave poles plays a crucial role in the convergence and accuracy of this new method. As the extraction of poles is required, a recently proposed algorithm by Teo *et al.* is also discussed and compared with existing methods in terms of computational speed.**

***Index Terms*—Discrete complex image method (DCIM), discrete complex image, Green's function, proper poles, Sommerfeld transform, surface-wave poles.**

I. Introduction

THE discrete complex image method (DCIM) is a widely used technique to convert the spectral-domain Green's function to a spatial-domain counterpart in the analysis of planar layered media. Basically, it is a semianalytical numerical technique to perform the Sommerfeld integral that arises in this conversion by using basis functions with known closed-form Sommerfeld transforms to represent the Green's functions.

For Green's functions with radial symmetry, the required integral is of the form

$$g(\rho) = \frac{1}{4\pi} \int_{\mathrm{SIP}} H_0^{(2)}(k_\rho \rho) G(k_\rho) k_\rho \, dk_\rho \tag{1}$$

where $H_0^{(2)}(\cdot)$ is the Hankel function of the second kind of order 0, "SIP" is the Sommerfeld integration path [11], $g(\rho)$ is the required spatial-domain Green's function, and $G(k_\rho)$ is its spectral-domain form.

For Green's functions that have $\cos\phi$ or $\sin\phi$ dependency, the integral can essentially be reduced to the following form:

$$g(\rho) = \frac{1}{4\pi} \int_{\mathrm{SIP}} H_1^{(2)}(k_\rho \rho) G(k_\rho) k_\rho^2 \, dk_\rho \tag{2}$$

where $H_1^{(2)}(\cdot)$ is the Hankel function of the second kind of order 1. The derivation of spectral-domain Green's functions is described in detail in [8] and is beyond the scope of this paper.

Manuscript received August 21, 2001; revised February 20, 2002.

S.-A. Teo is with Marvell Inc., Sunnyvale, CA 94089 USA (e-mail: teosweeann@ieee.org).

S.-T. Chew is with the Defence Science Organization National Laboratories, Singapore 118230 and also with the Microwave Division, Department of Electrical and Computer Engineering, National University of Singapore, Singapore 119260.

M.-S. Leong is with the Microwave Division, Department of Electrical and Computer Engineering, National University of Singapore, Singapore 119260.

Digital Object Identifier 10.1109/TMTT.2002.807834

The numerical form of the DCIM was originally proposed by Chow *et al.* in [3], where he partitioned the Green's function of microstrip structures using the following approximation:

$$G(k_\rho) \cong G_q(k_\rho) + G_{\mathrm{sw}}(k_\rho) + G_{\mathrm{residue}}(k_\rho) \tag{3}$$

where $G_q(k_\rho)$ is the quasi-static image of $G(k_\rho)$, which satisfies

$$G_q(k_\rho) = \lim_{k_0 \to 0} G(k_\rho) \tag{4}$$

where k_0 is the wavenumber. Physically, the quasi-static image represents the contribution of the Green's function in the near-field region.

The second term $G_{\mathrm{sw}}(k_\rho)$ represents the surface-wave contribution that are associated with the poles of the spectral-domain Green's function. Since the poles occur in pairs where one is the negative of the other, they can be written as

$$G_{\mathrm{sw}}(k_\rho) = \sum_{i=1}^{N} \frac{2a_i p_i}{k_\rho^2 - p_i^2} \tag{5}$$

where p_i are the locations of the poles in the complex k_ρ domain and a_i are the residues of these singularities. It can be shown that, when transformed to the spatial domain, $G_{\mathrm{sw}}(k_\rho)$ provides the dominant contribution in the far-field region, i.e., for large ρ, given that the Green's function does indeed contain at least one pole [10].

Finally, the last term $G_{\mathrm{residue}}(k_\rho)$ approximates $[G(k_\rho) - G_q(k_\rho) - G_{\mathrm{sw}}(k_\rho)]$ using the series

$$G_{\mathrm{residue}} = \sum_{i=1}^{N} A_i \frac{\exp(-jk_z c_i)}{2jk_z} \tag{6}$$

where $k_z^2 = k_0^2 - k_\rho^2$ and the coefficients A_i and c_i are to be obtained using the Prony's method.

After approximating the spectral-domain Green's function using (3), an approximate spatial-domain Green's function can be obtained as all the right-hand side (RHS) terms, the expression have closed-form Sommerfeld transforms by applying Cauchy's residues theorem to $G_{\mathrm{sw}}(k_\rho)$

$$\begin{aligned} g_{\mathrm{sw}}(\rho) &= \frac{1}{4\pi} \int_{\mathrm{SIP}} H_0^{(2)}(k_\rho \rho) G_{\mathrm{sw}}(k_\rho) k_\rho \, dk_\rho \\ &= -\frac{j}{2} \sum_{i=1}^{N} a_i H_0^{(2)}(p_i \rho) \end{aligned} \tag{7}$$

and the Sommerfeld identity to $G_q(k_\rho)$ and $G_{\text{residue}}(k_\rho)$

$$\frac{1}{4\pi}\int_{\text{SIP}} H_0^{(2)}(k_\rho\rho)\frac{\exp(-jk_z c)}{2jk_z}\,k_\rho\,dk_\rho = \frac{\exp(-jk_0\sqrt{\rho^2+c^2})}{4\pi\sqrt{\rho^2+c^2}} \quad (8)$$

where $\Im[k_z] \le 0$ due to Sommerfeld's radiation condition and $\Re[c] \ge 0$ for convergence.

After Chow *et al.*'s original contributions, the DCIM technique was improved by Aksun, who proposed a robust two-level GPOF technique for extracting the residues [2]. Besides this difference, the poles of the spectral-domain Green's functions are not extracted; the spectral-domain Green's function is approximated using the following:

$$G(k_\rho) \cong G_q(k_\rho) + G_{\text{residue}}(k_\rho) \quad (9)$$

where $G_{\text{residue}}(k_\rho)$ is obtained using the two-level generalized pencil of function (GPOF) technique [2].

As the poles are not extracted, it is noted that the resulting approximation will not be accurate in the far-field region. However, there are several benefits accorded due to this. First, by not extracting the poles, the new technique becomes suitable for multilayered structures as the logarithmic singularity at $\rho = 0$ associated with $g_{\text{sw}}(\rho)$ in (7), due to the Hankel functions, is removed. With the exception where $z = z'$, the spatial-domain Green's functions are, in general, bounded at $\rho = 0$.

Another advantage of not extracting surface-wave poles is due to the difficulty of locating the poles of the Green's function.

Ling *et al.* has also noted that the Green's function obtained using this technique is not accurate in the far-field region and proposed that two Green's functions should be derived so that both the near field (Aksun's) and far field (Chow's) can be represented accurately [4].

However, as two Green's functions are required, the computational complexity increases. For instance, one would need to interpolate between the two Green's functions over an intermediate region (between the far and near fields).

To resolve this, Teo *et al.* took an alternative method by deriving a single Green's function that is able to approximate both the near and far fields [1]. In this paper, the author will present an error analysis of the DCIM technique proposed in [1]. As pole extraction is required in this technique, the pole-extraction method in [1] will also be discussed.

II. Theory

In all DCIM techniques, one is primarily concerned with evaluating, in closed form, the Sommerfeld integral. It can be seen from the previous section that, despite the differences in $G_{\text{residue}}(k_\rho)$ and on whether the poles are to be extracted, the DCIM techniques are based on the same principle: the user seeks the function $G_{\text{residue}}(k_\rho)$ to represent a certain portion of the Green's function by using the following series:

$$G_{\text{residue}} = \sum_{i=1}^{N} A_i \frac{\exp(-jk_z c_i)}{2jk_z} \quad (10)$$

so that it can be transformed to the spatial domain by using (8). For Green's function of the form shown in (2), one could use the following series:

$$G_{\text{residue}}(k_\rho) = \sum_{i=1}^{N} A_i \frac{\exp(-jk_z c_i)}{k_\rho^2} \quad (11)$$

so that it can be transformed using the following identity:

$$\frac{1}{4\pi}\int_{\text{SIP}} H_1^{(2)}(k_\rho\rho)\frac{\exp(-jk_z c)}{k_\rho^2}\,k_\rho^2\,dk_\rho = \frac{1}{2\pi\rho}\left[\exp(-jk_0 c) - c\frac{\exp\left(-jk_0\sqrt{\rho^2+c^2}\right)}{\sqrt{\rho^2+c^2}}\right]. \quad (12)$$

To analyze the error performance, it is first noted that the accuracy of the methods depends solely on validity and accuracy of the approximation $G_{\text{residue}}(k_\rho) \cong G(k_\rho) - G_q(k_\rho)$ in Aksun's method and of $G_{\text{residue}}(k_\rho) \cong G(k_\rho) - G_q(k_\rho) - G_{\text{sw}}(k_\rho)$ in Chow *et al.*'s method.

Assuming the Green's function $G(k_\rho)$ does contain at least one surface-wave pole then, for large values of ρ, $g(\rho)$ will be dominated by the Cauchy residues of these poles

$$\lim_{\rho\to\infty}\frac{1}{4\pi}\int_{\text{SIP}} G(k_\rho)H_n^{(2)}(k_\rho\rho)k_\rho^{n+1}\,dk_\rho = -\frac{j}{2}\sum_{i=1}^{N} a_i p_i^{n+1} H_n^{(2)}(p_i\rho). \quad (13)$$

where "SIP" is the Sommerfeld integration path and a_i are the residues of the poles located at the points p_i in the lower half of the complex k_ρ-plane.

Hence, knowing that surface-wave propagation within lossless substrates decays at a rate of $\rho^{-1/2}$, it is obvious that, for such cases, if these poles are not extracted and represented in terms of Hankel functions, the discrete complex images are not sufficient since they have exponential decay or ρ^{-1} decay.

As for Chow *et al.*'s method, the Green's function is accurately represented in the far-field region, as in this method, these poles are to be extracted as $G_{\text{sw}}(k_\rho)$, as discussed in the previous section.

However, in the near-field region, since the Hankel functions contain logarithmic singularities at $\rho = 0$, which $G_{\text{residue}}(k_\rho)$ does not have, it is clear that, in Chow *et al.*'s method, the derived spatial Green's functions would not be accurate near $\rho = 0$, unless the Green's function is indeed singular at $\rho = 0$. This was indeed the case, in Chow *et al.*'s paper, when he considered Green's functions of microstrip structures, for the case of $z = z'$, which have a $1/\rho$ singularity at $\rho = 0$.

The reason for this phenomenon is easier to explain in the spectral domain. The complex images need to approximate $[G(k_\rho) - G_q(k_\rho) - G_{\text{sw}}(k_\rho)]$; for large k_ρ, the dominant term $G_{\text{sw}}(k_\rho)$ decays at a rate of k_ρ^{-2}, while the discrete complex images in the spectral domain have exponential decay. Hence, the complex images are not able to approximate the slow decay well.

To solve this problem, Teo *et al.* [1] proposed to extract the quasi-static image of the surface-wave poles using a term

$G_{\rm swq}(k_\rho)$, which has the property that $[G_{\rm sw}(k_\rho)+G_{\rm swq}(k_\rho)]$ decays at a rate of at least k_ρ^{-4} or k_ρ^{-8}.

It can be shown that with (5), if $G_{\rm swq}(k_\rho)$ is given by the following:

$$G_{\rm swq}(k_\rho)=-\frac{\sum_{i=1}^{N}2a_ip_i}{k_\rho^2+\sum_{i=1}^{N}p_i^2} \tag{14}$$

then, $(G_{\rm sw}+G_{\rm swq})$ will decay at a rate of k_ρ^{-4}.

Alternatively, if one chooses

$$G_{\rm swq}(k_\rho)=-\frac{\sum_{i=1}^{N}2a_ip_i}{k_\rho^2+\sum_{i=1}^{N}p_i^2} -\frac{\left(\sum_{i=1}^{N}2a_ip_i\right)\left(\sum_{i=1}^{N}p_i^2\right)+\sum_{i=1}^{N}2a_ip_i^3}{k_\rho^4+(1/2)\left[\left(\sum_{i=1}^{N}p_i^2\right)^2+\sum_{i=1}^{N}p_i^4\right]} \tag{15}$$

then $(G_{\rm sw}+G_{\rm swq})$ will have a decay of k_ρ^{-8}.

Hence, it is proposed that the spectral-domain Green's function should be approximated using

$$G(k_\rho)\cong G_q(k_\rho)+G_{\rm sw}(k_\rho)+G_{\rm swq}(k_\rho)+G_{\rm residue}(k_\rho) \tag{16}$$

where $G_{\rm residue}(k_\rho)$ is to be obtained using the two-level GPOF method applied to $G_{\rm residue}(k_\rho)=G(k_\rho)-G_q(k_\rho)-G_{\rm sw}(k_\rho)-G_{\rm swq}(k_\rho)$, as described in [2].

The Sommerfeld transform of $G_{\rm swq}(k_\rho)$ can easily be affected by expanding $G_{\rm swq}(k_\rho)$ into partial fractions and applying Cauchy's residue theorem to them; the treatment of $G_{\rm swq}(k_\rho)$ is, in fact, no different from that of surface-wave poles.

Even though $G_{\rm residue}(k_\rho)$ in this proposed technique still decays exponentially and does not model the polynomial decay of the $[G_{\rm sw}(k_\rho)+G_{\rm swq}(k_\rho)]$ well, the error of this approximation is greatly reduced due to the faster decay of the latter.

The convergence of this new DCIM for Green's functions with radial symmetry can be analyzed by deriving the error expressions. Assuming that, for large $k_\rho\geq a$, the dominant term of the approximate Green's function is given by $G_{\rm sw}(k_\rho)$ or $G_{\rm swq}(k_\rho)$, then for

$$\begin{aligned} k_\rho>a,\ &\left[G(k_\rho)-G_q(k_\rho)-G_{\rm sw}(k_\rho)\right.\\ &\left.-G_{\rm swq}(k_\rho)-G_{\rm residue}(k_\rho)\right]\\ &\cong -G_{\rm sw}(k_\rho)-G_{\rm swq}(k_\rho)\\ &\cong\begin{cases}Ak_\rho^{-2}, & G_{\rm swq}(k_\rho)=0\\ Ak_\rho^{-4}, & \text{(14) is used}\\ Ak_\rho^{-8}, & \text{(15) is used}\end{cases}\end{aligned} \tag{17}$$

where A is a constant.

Therefore, the error is given by the following integral:

$$\begin{aligned}\mathcal{E}_n(a,\rho)&=\frac{1}{2\pi}\int_0^\infty J_0(k_\rho\rho)\left[G-G_q-G_{\rm sw}-G_{\rm swq}\right]k_\rho\,dk_\rho\\ &=\frac{1}{2\pi}\int_0^a J_0(k_\rho\rho)[G-G_q-G_{\rm sw}-G_{\rm swq}]k_\rho\,dk_\rho\\ &\quad+\frac{A}{2\pi}\int_a^\infty J_0(k_\rho\rho)k_\rho^{1-n}\,dk_\rho.\end{aligned} \tag{18}$$

Assuming that, for $k_\rho\leq a$, $G_{\rm residue}(k_\rho)$ is a good approximation for the residual terms, then

$$\frac{1}{2\pi}\int_0^a J_0(k_\rho\rho)[G-G_q-G_{\rm sw}-G_{\rm swq}]k_\rho\,dk_\rho\cong 0. \tag{19}$$

Therefore,

$$\mathcal{E}_n(a,\rho)\cong\frac{A}{2\pi}\int_a^\infty J_0(k_\rho\rho)k_\rho^{1-n}\,dk_\rho \tag{20}$$

where $n=2$ if $G_{\rm swq}=0$; $n=4$ if (14) is used, and $n=8$ if (15) is used. For simplicity, the value of A shall be assumed to be equal to 2π in the remainder of this paper.

Similarly, in the error for Green's function, which have $\cos\phi$ or $\sin\phi$ dependencies, the error function can be approximated using

$$\mathcal{D}_n(a,\rho)=\int_a^\infty J_1(k_\rho\rho)k_\rho^{2-n}\,dk_\rho. \tag{21}$$

For Green's functions of this form, if $G_{\rm swq}(k_\rho)=0$, then the resulting error is given by $\mathcal{D}_2(a,\rho)$; if (14) or equation (15) are used, then the errors are given by $\mathcal{D}_4(a,\rho)$ and $\mathcal{D}_8(a,\rho)$, respectively.

Both the error functions as shown in (20) and (21) have closed-form solutions; with $G_{\rm swq}=0$, the error functions are given by the following with $n=2$:

$$\mathcal{E}_2(a,\rho)=\frac{a^2\rho^2}{8}\,{}_2F_3(1,1;2,2,2,-a^2\rho^2/4)-\gamma+\log\frac{2}{\rho a} \tag{22}$$

$$\mathcal{D}_2(a,\rho)=\frac{J_0(a\rho)}{\rho} \tag{23}$$

where $\gamma=0.577216$ is the Euler's constant and F is the generalized hypergeometric function.

A. Choice of $G_{\rm swq}$ for Green's Functions With Radial Symmetry

It can be seen that, without extracting the quasi-static image of $G_{\rm sw}$, the corresponding error function $\mathcal{E}_2(a,\rho)$ is singular at $\rho=0$ regardless of the value of a. This implies that the complex images produce inaccurate results for small ρ, which agrees with the conclusions drawn in the previous section.

Fortunately, if the quasi-static image of the surface-wave poles is extracted such that $(G_{\rm sw}+G_{\rm swq})$ has a decay corresponding to k_ρ^{-4} or k_ρ^{-8}, the error functions can be made sufficiently small by a suitable choice of a.

From Figs. 1 and 2, it can be observed that $\mathcal{E}_8(a,\rho)$ has much better performance than $\mathcal{E}_4(a,\rho)$. In practice, it was found that, despite this fact, using (14) is usually sufficient, as the value of

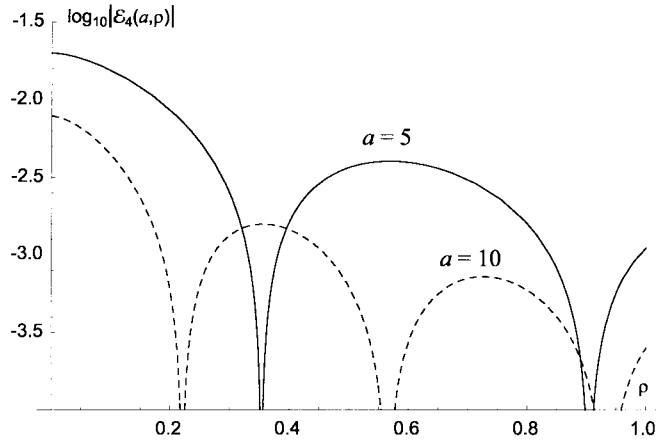

Fig. 1. Plot of $\log_{10}|\mathcal{E}_4(5,\ \rho)|$ and $\log_{10}|\mathcal{E}_4(10,\ \rho)|$ against ρ.

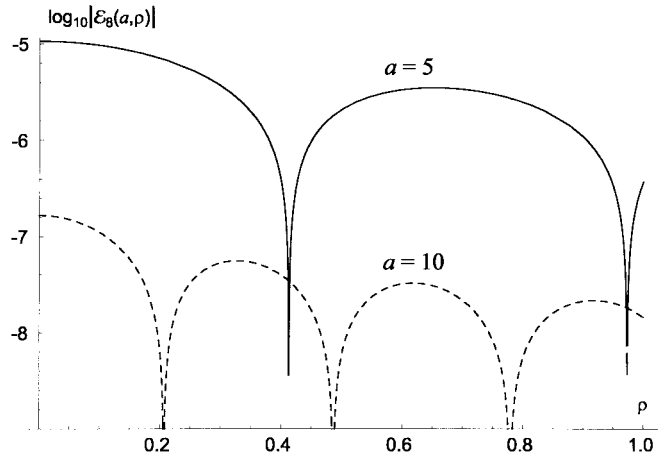

Fig. 2. Plot of $\log_{10}|\mathcal{E}_8(5,\ \rho)|$ and $\log_{10}|\mathcal{E}_8(10,\ \rho)|$ against ρ.

a is usually much larger than those shown here. It can easily be shown by using Schwartz's inequality that, for fixed ρ, $\mathcal{E}_4(a,\ \rho)$ decays faster than a^{-2}. However, this would mean more complex image terms.

For the error to remain negligible as ρ increases, one has to ensure that the error function decays faster than the Green's function. Since the slowest decaying function in the spatial-domain Green's function is the Hankel function, which decays at a rate of $\rho^{-1/2}$, this is not a difficult requirement to meet. It was found numerically that $\mathcal{E}_n(a,\ \rho)$ decays at a rate of $\rho^{-3/2}$ for $n \geq 2$ and, hence, this requirement has also been also met.

III. Choice of G_{swq} for Green's Functions With $\sin\phi$ or $\cos\phi$ Dependencies

For Green's functions with $\sin\phi$ or $\cos\phi$ dependencies, it can be observed from (23) that $\mathcal{D}_2$, the error function corresponding to the case where $G_{\mathrm{swq}} = 0$, is also singular at $\rho = 0$. Therefore, like the previous case, this means that the obtained spatial-domain Green's function would be inaccurate for small ρ.

Therefore, one needs to examine if the error can be removed by using a suitable function to represent the quasi-static image

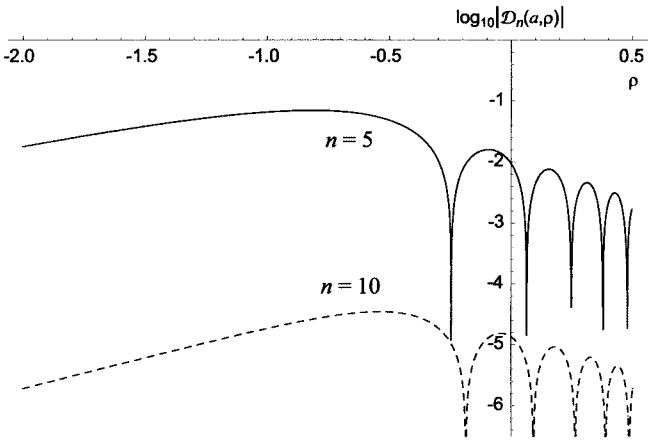

Fig. 3. Plot of $\log_{10}|\mathcal{D}_4(5,\ \rho)|$ and $\log_{10}|\mathcal{D}_8(5,\ \rho)|$ against ρ.

of G_{sw}. The series expansions of the relevant error functions for small ρ for $\mathcal{D}_4(a,\ \rho)$ and $\mathcal{D}_8(a,\ \rho)$ give

$$\begin{aligned}\mathcal{D}_4(a,\ \rho) &= \frac{\rho}{32}\left[a^2\rho^2\,{}_2F_3(1,\ 1;\ 2,\ 2,\ 3;\ -a^2\rho^2/4)\right.\\ &\qquad\left.+\ 8\left(1-2\gamma+2\ln\frac{2}{a\rho}\right)\right]\\ &= \frac{\rho}{4}\left(1-2\gamma+2\ln\frac{2}{a\rho}\right)+\frac{a^2\rho^3}{32}+\cdots \qquad (24)\end{aligned}$$

$$\begin{aligned}\mathcal{D}_8(a,\ \rho) &= \frac{\rho}{36e864a^4}\left\{a^6\,\rho^6\,{}_2F_3(1,\ 1;\ 2,\ 4,\ 5;\ -a^2\rho^2/4)\right.\\ &\qquad -16\left[-288+72a^2\rho^2\right.\\ &\qquad\quad +a^4\rho^4(-10+6\gamma-3\ln 4)\\ &\qquad\quad \left.\left.+\ 6a^4\rho^4\ln a\rho\right]\right\}\\ &= \frac{\rho}{8a^4}-\frac{\rho^3}{32a^2}+\frac{\rho^5}{1152}\left(5-3\gamma+3\ln\frac{2}{a\rho}\right)+\cdots. \qquad (25)\end{aligned}$$

It can be seen from (24) that (14) is not a good candidate for G_{swq}. This is because of the logarithmic singularity of both a and ρ embedded in the coefficients of ρ in $\mathcal{D}_4$.

Fortunately, further investigation of (25) shows that (15) gives good convergence for all ρ. It was found numerically that $\mathcal{D}_8(a,\ \rho)$ also decays at a rate of $\rho^{-3/2}$. Hence, it also satisfies the requirement that the error function must decay faster than the Hankel function. A comparison of $\mathcal{D}_4(a,\ \rho)$ and $\mathcal{D}_8(a,\ \rho)$ in Fig. 3 shows that $\mathcal{D}_8$ is much smaller than $\mathcal{D}_4$.

IV. Pole Extraction

In this proposed DCIM, the complete knowledge of the locations of poles in the Green's function is critical. Many pole-extraction techniques have been proposed by various authors, but they usually have a limited range of application or are computationally expensive.

For simple geometries, such as single-layered structures, a commonly used techniques used for locating the poles is to apply the modified Newton–Raphson algorithm on the characteristics equations of the geometry. Another method proposed

by Teo *et al.* [9] uses contraction mapping to find the solutions of the TE and TM characteristics equations of a grounded dielectric slab. However, both of these methods are limited to single-layered structures.

For more complicated geometries, finding suitable starting points for the Newton–Raphson algorithm is often difficult. Recently, Ling *et al.* [4] has also proposed a method that extracts the poles by recursively performing contour integrals to find the locations of these poles. The main drawback of this method is that it requires a large number of sampling points in the integral when the contour lies too close to a pole, and which is inherently inevitable in this method.

A more general method was proposed in [1]; this method does not need to integrate near the poles and the computation requirement is equivalent to that of a single contour integral. In this section, a brief description of this method is given and comparison of this method is made against two other methods proposed in existing literature [4], [9].

A. Algorithm

First, a suitable contour C should be chosen such that C encloses all the poles of this Green's function. Having selected the contour, the following series shall be constructed next:

$$T_n = \int_C G(k_\rho) \exp\left[ns(k_\rho - q)\right] dk_\rho \tag{26}$$

for $n = 0, 1, 2, \ldots, M-1$, where M is greater than twice the number of poles that is located within the contour, s is a scaling factor, and q is a constant offset. Care should be taken to avoid the branch-cut of the Green's function or, if needed, it can be removed by a suitable change of variable.

By applying the Cauchy's residues theorem, one obtains

$$T_n = 2\pi j \sum_{i=1}^{N} a_i \exp\left[ns(p_i - q)\right] \tag{27}$$

where p_i are the locations of the poles, a_i are the residues of the poles, and N is the total number of poles.

To prevent numerical overflow or underflow, q is chosen to be the point that lies approximately in the center of C. In a numerical routine, one could set it to

$$q = \frac{\oint_C k_\rho |dk_\rho|}{\oint_C |d\rho|} \tag{28}$$

as this will give the center of the contour C.

To further optimize the method, it is noted that $\exp[ns(k_\rho - q)]$ has a real exponential dependency when k_ρ varies in the direction where $s\,\Delta k_\rho$ is a real number and have a complex exponential dependency when Δk_ρ is complex. It is advantageous to reduce the real exponential dependency and increase the complex exponential behavior. Therefore, for simplicity, one should pick two points w_1, $w_2 \in C$ such that w_1 and w_2 are the furthest apart from each other, and pick s such that

$$\Re[(w_1 - w_2)s] = 0 \tag{29}$$

$$|(w_1 - w_2)s| = \pi. \tag{30}$$

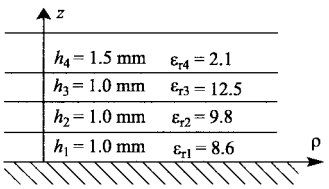

Fig. 4. Geometry of the four-layer grounded structure analyzed in this paper.

The computational cost of evaluating the M integrals in the form of (26) can be greatly reduced since the contours for every integral is the same and the only term that is changed within the integrand is the exponential term. Hence, by writing

$$\mathbf{T} = \int_C G(k_\rho)\mathbf{E}(k_\rho)\, dk_\rho \tag{31}$$

where

$$\mathbf{E}(k_\rho) = \begin{pmatrix} 1 \\ \exp[s(k_\rho - q)] \\ \exp[2s(k_\rho - q)] \\ \vdots \\ \exp\left[(M-1)s(k_\rho - q)\right] \end{pmatrix} \tag{32}$$

the M integrals can be integrated simultaneously as a single integral.

Since T_n as shown in (27) is a series consisting of a sum of exponentials terms, the GPOF technique can be used to calculate the values of a_i and p_i as long as $M \geq 2N$ [2], [6]. Due to the finite precision used, the poles obtained using the GPOF extraction may contain some error and should be further refined using the modified Newton–Raphson method using these points as the initial solutions. Finally, to ensure that all the poles have been extracted, the algorithm is to be reiterated with the known poles extracted until no pole is to be found.

V. Numerical Results

A. Pole Extraction

In this section, some numerical results shall be present. The results validate the accuracy of both the pole-extraction algorithm and the proposed DCIM. The geometry used in this paper has four layers and a ground plane. The relative permittivities and thickness of each layer are as shown in Fig. 4 and $k_0 = 2\pi 30 \times 10^9 \sqrt{\epsilon_0 \mu_0}$.

By using the proposed pole-extraction algorithm, the TE and TM poles of the mixed potential Green's functions (formulation C) [8] are as follows:

$$\text{TE: } k_r = \{1878.12,\ 1103.23\} \tag{33}$$

$$\text{TM: } k_r = \{661.46,\ 1351.89,\ 1875.14\}. \tag{34}$$

In order to extract the TE poles, G_{xx} was used since it contain only TE poles. G_{zx} contains both TE and TM poles and, hence, the TE poles were extracted first, before the algorithm was used. The amount of computation time for extracting the poles was less than 1 min with the algorithm programmed in MATLAB and running on a Pentium III 800-MHz processor.

TABLE I
COMPARISON OF COMPUTATION TIME TAKEN FOR POLE EXTRACTION USING CURRENT ALGORITHM AGAINST OTHER ALGORITHMS PROPOSED IN [4] AND [9] FOR GREEN'S FUNCTIONS WITH A VARIOUS NUMBER OF POLES

No of poles	$\frac{\text{time using [4]}}{\text{time using [1]}}$	$\frac{\text{time using [9]}}{\text{time using [1]}}$
2	3.5	0.12
3	5.6	0.087
4	9.8	0.046
5	15.7	0.031
6	25.6	0.025

This algorithm was compared against two other algorithms proposed in [4] and [9]. The results are as shown in Table I. In the case of [9], the comparison is made only for the case of a grounded dielectric slab.

B. DCIM

Next, the various DCIM techniques were used to compute the spatial-domain form of G_{zx}.

In Figs. 5–8, the near- and far-field performances of the DCIM techniques using various choices of $G_{\rm sw}(k_\rho)$ and $G_{\rm swq}(k_\rho)$ are shown and compared against results obtained using numerical integration. In these figures, unless stated otherwise, $G_{\rm sw}(k_\rho)$ is not equal to zero and is as given in (5).

In these figures, the case where $G_{\rm sw}(k_\rho) = 0$ corresponds to Aksun's method, and the case where $G_{\rm swq}(k_\rho) = 0$ corresponds to Chow *et al.*'s method, except that the two-level GPOF method is used to extract the complex images instead of Prony's method, as originally proposed.

Finally, a summary of the number of image terms and Hankel functions used by each method is presented in Table II for the example shown in Figs. 5 and 6. Similar results were obtained for the example shown in Figs. 7 and 8, though they are not presented.

VI. DISCUSSION

A. Pole Extraction

A comparison between the pole-extraction method proposed in [1], [4], and [9] is made and shown in Table I. The results show that the method proposed in [1] is much faster than the method proposed in [4]. This is because when the number of poles increases, the number of integrals that are required does not increase for the former, whereas for the latter, it increases approximately linearly. In the latter, additional complications also arise when the contour integrals are taken too close to the poles.

In the case where the geometry is a grounded dielectric slab, the current method is much slower than that proposed in [9]. This is because the method in [9] does not even require any numerical integration. However, the drawback is it is valid only for this geometry and, hence, not as general as the current method.

B. DCIM

In Fig. 5, the near-field performances of DCIM methods applied to a Green's function whose value at the origin is zero are compared against results obtained using numerical integration. It can be seen that when $G_{\rm sw}(k_\rho) = 0$ and $G_{\rm swq}(k_\rho) = 0$, the near field is accurate. However, when the surface-wave poles are included and $G_{\rm swq}(k_\rho) = 0$, the results for small a diverges. When (14) is used for $G_{\rm swq}(k_\rho)$, the results improve slightly; there is some divergence for small a. This is as predicted in the error analysis done in the previous section. Finally, when (15) is used for $G_{\rm swq}(k_\rho)$, it is observed that the results are convergent in the near-field region.

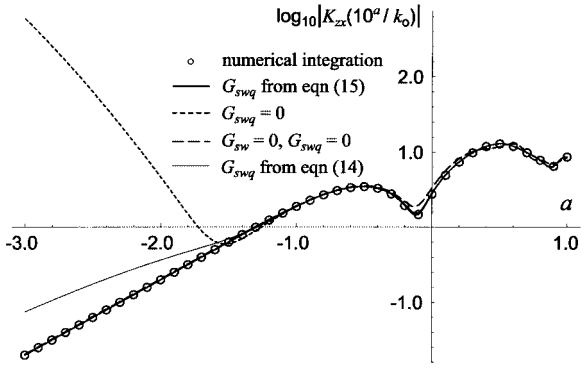

Fig. 5. Plot of $\log_{10}|G_{zx}(10^a/k_0)|$ with respect to a for $-3.0 < a < 1.0$ for $z = 0.5 \times 10^{-3}$ and $z' = 1 \times 10^{-3}$ for different $G_{\rm sw}(k_\rho)$ and $G_{\rm swq}(k_\rho)$.

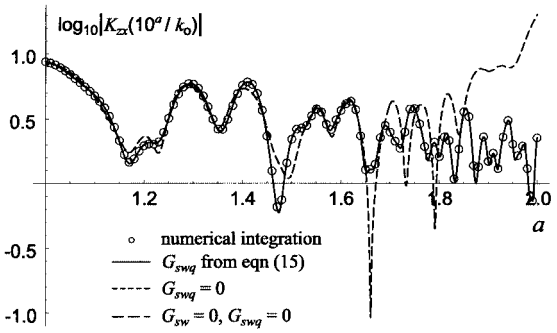

Fig. 6. Plot of $\log_{10}|G_{zx}(10^a/k_0)|$ with respect to a for $1.0 < a < 2.0$ for $z = 0.5 \times 10^{-3}$ and $z' = 1 \times 10^{-3}$ for different $G_{\rm sw}(k_\rho)$ and $G_{\rm swq}(k_\rho)$.

In Fig. 6, the far-field performances of the DCIM techniques applied to same Green's function is shown. In this example, only the case where $G_{\rm sw}(k_\rho) = 0$ is divergent. This is because, in the far-field region, the surface-wave poles are the dominant contributions.

In Fig. 7, the near-field performances are shown for the case where the Green's function is singular at the origin. It is observed that, unlike Fig. 5, extracting $G_{\rm sw}(k_\rho)$, but setting $G_{\rm swq}(k_\rho) = 0$ does not affect the results as much. The reason is, even though doing so causes error, the singularity of the Green's function is more dominant than that of the error function. Hence, this validates the original intended applications of Chow *et al.*'s method for Green's functions, which are singular at the original in the spatial domain. Some errors are observed for the case where $G_{\rm sw}(k_\rho) = 0$ and $G_{\rm swq}(k_\rho) = 0$ for $a > 0$. The current method is, on the other hand, accurate throughout this range.

In Fig. 8, the far-field performances of the same Green's function are shown. The results show again that, in the far-field

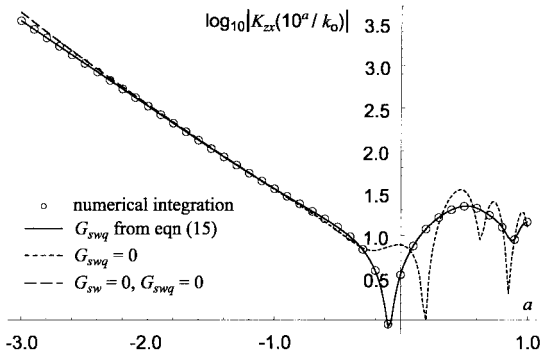

Fig. 7. Plot of $\log_{10}|G_{zx}(10^a/k_0)|$ with respect to a for $-3.0 < a < 1.0$ for $z = z' = 1 \times 10^{-3}$ for different $G_{\rm sw}(k_\rho)$ and $G_{\rm swq}(k_\rho)$.

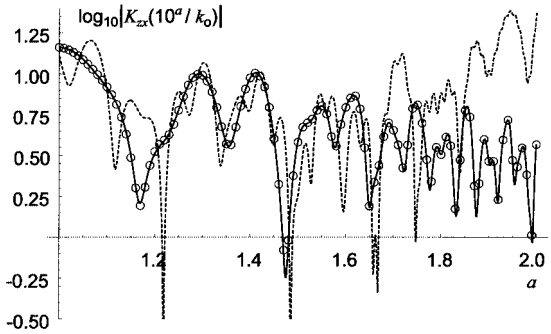

Fig. 8. Plot of $\log_{10}|G_{zx}(10^a/k_0)|$ with respect to a for $1.0 < a < 2.0$ for $z = z' = 1 \times 10^{-3}$ for different $G_{\rm sw}(k_\rho)$ and $G_{\rm swq}(k_\rho)$ (refer to Fig. 7 for legend).

TABLE II
COMPARISON OF THE NUMBER OF IMAGE TERMS IN $[G_{\rm residue} + G_q]$ AND THE NUMBER OF HANKEL FUNCTIONS IN $[G_{\rm sw} + G_{\rm swq}]$ FOR THE DIFFERENT METHODS FOR THE CASE SHOWN IN FIGS. 5 AND 6

method	No of terms	
	$G_{\rm residue} + G_{\rm q}$	$G_{\rm sw} + G_{\rm swq}$
$G_{\rm sw} = 0$ and $G_{\rm swq} = 0$	24	0
$G_{\rm swq} = 0$	9	5
$G_{\rm swq}$=eqn (14)	9	6
$G_{\rm swq}$=eqn (15)	9	8

region, the DCIM techniques are accurate only if the poles are extracted.

Overall, it is found that Aksun's method ($G_{\rm sw}(k_\rho) = 0$ and $G_{\rm swq}(k_\rho) = 0$) is accurate in the near-field region. Chow *et al.*'s method is always accurate in the far-field region and is also accurate in the near-field region when the Green's function is singular at the origin. Teo *et al.*'s method is the only method that is accurate in both the far- and near-field regions.

In Table II, the number of terms that are required by each method to construct the Green's function is shown. Overall, Aksun's method ($G_{\rm sw}(k_\rho) = 0$ and $G_{\rm swq}(k_\rho) = 0$) requires the most terms. However, it does not require any Hankel functions. As Hankel functions are somewhat more difficult to calculate accurately than the exponential image functions, it is difficult to ascertain which is more computationally efficient.

The number of image terms decreases rapidly when the poles are extracted. Comparing Teo *et al.*'s method with Chow *et al.*'s method, it requires one or three additional Hankel functions depending on the choice of $G_{\rm swq}(k_\rho)$.

VII. CONCLUSION

A complete error analysis of the various DCIM techniques has been performed and it has shown that the DCIM technique presented in [1] is able to obtain spatial Green's functions that are accurate in both the near and far fields. Guidelines on the selection of $G_{\rm swq}(k_\rho)$ have also been given. A comparison of the efficiency of the various pole-extraction algorithms shows that, except for specific geometries, Teo *et al.*'s pole extraction was the most efficient and robust.

It was found that, by using the pole-extraction and DCIM techniques proposed in [1], a robust and efficient algorithm to perform the Sommerfeld transform was obtained.

REFERENCES

[1] S.-A. Teo *et al.*, "A robust generalized DCIM technique with pole extraction," in *IEEE AP-S Int. Symp.*, vol. 4, July 2001, pp. 862–864.
[2] M. I. Aksun, "A robust approach for the derivation of closed-form Green's functions," *IEEE Trans. Microwave Theory Tech.*, vol. 44, pp. 651–658, May 1996.
[3] Y. L. Chow *et al.*, "A closed-form spatial Green's function for thick microstrip substrate," *IEEE Trans. Microwave Theory Tech.*, vol. 39, pp. 588–592, Mar. 1991.
[4] F. Ling *et al.*, "Discrete complex image method for Green's functions of general multilayer media," *IEEE Microwave Guided Wave Lett.*, vol. 10, pp. 400–402, Oct. 2000.
[5] W. C. Chew, *Waves and Fields in Inhomogeneous Media*. New York: Van Nostrand, 1990.
[6] Y. Hua and T. K. Sarkar, "Generalized pencil-of-function method for extracting poles of an EM system from its transient response," *IEEE Trans. Antennas Propagat.*, vol. 37, pp. 229–234, Feb. 1989.
[7] D. B. Webb and R. Mittra, "Practical implementation of the complex image method for the solution of nonplanar multilayered media problems," in *IEEE AP-S Int. Symp.*, vol. 1, July 1996, pp. 420–423.
[8] K. A. Michalski and D. Zheng, "Electromagnetic scattering and radiation by surfaces of arbitrary shape in layered media—Part I: Theory," *IEEE Trans. Antennas Propagat.*, vol. 38, pp. 335–344, Mar. 1990.
[9] S.-A. Teo *et al.*, "Complete location of poles for thick lossy grounded dielectric slab," *IEEE Trans. Microwave Theory Tech.*, vol. 50, pp. 440–445, Feb. 2002.
[10] N. Bleistein and R. A. Handelsman, *Asymptotic Expansions of Integrals*. New York: Dover, 1975.
[11] A. Sommerfeld, *Partial Differential Equations in Physics*. New York: Academic, 1949.

Swee-Ann Teo (S'00–M'01) received the B.Eng. degree (with first-class honors and vice-chancellor list) in electrical engineering and M.Eng. degree from the National University of Singapore, Singapore, in 1999 and 2001, respectively.

He was a Research Scholar with the National University of Singapore. In 2001, he joined the Wireless Connectivity Division, Microtune Inc. (formerly Transilica Inc.), where he was involved with integrated CMOS voltage-controlled oscillators (VCOs), and phase-locked loops (PLLs) for wireless applications. He is currently with Marvell Inc., Sunnyvale, CA, as an RFIC Engineer involved with wireless systems. His research interests include integral-equation methods, fast multipole methods and DCIMs, low-noise oscillators, and nonlinear circuits.

Mr. Teo was the recipient of a grant presented by the Defence Science Organization (DSO) National Laboratories, Singapore.

Siou-Teck Chew (S'94–M'96) received the B.Eng. (with honors) and M.Eng. degrees from the National University of Singapore (NUS), Singapore, in 1989 and 1993, respectively, and the Ph.D. degree from the University of California at Los Angeles (UCLA), in 1996.

Since 1989, he has been with the Defence Science Organization (DSO) National Laboratories, Singapore, where he is currently the Center Head (Advanced Electronics and Signal Processing) and a Distinguished Member of Technical Staff. He oversees the research and development of digital and microwave components and subsystems and advanced signal processing. He is currently and Adjunct Associate Professor with the Microwave Division, Department of Electrical and Computer Engineering, NUS, where he lectures and supervises research activities. His technical interests include active antennas, high-power amplifiers, filters and nonlinear circuit analysis and design. He has authored or coauthored 20 papers and one book.

Dr. Chew is the chairman of the IEEE Singapore Chapter for Antennas and Propagation (AP)/Microwave Theory and Techniques (MTT)/Electromagnetic Compatibility (EMC) (2000–2001). He was the recipient of a Defence Technology Training Award (DTTA) Scholarship presented by the Ministry of Defence, Singapore.

Mook Seng Leong (M'75–SM'98) received the B.Sc. in engineering (with first-class honors) and Ph.D. degree in microwave engineering from the University of London, London, U.K., in 1968 and 1971, respectively.

From 1971 to 1973, he was a Post-Doctoral Research Fellow with Queen Mary College, University of London, where he investigated high-efficiency microwave antennas in collaboration with Andrew Antennas, Lochgelly, U.K., and Microwave Associates, Luton, U.K. In 1973, he joined the National University of Singapore, Singapore, and is currently a Professor and Head of the Microwave and RF Group, Electrical and Computer Engineering Department. He has authored or coauthored over 150 technical papers in international journals and has consulted extensively by statutory boards and public and private companies. He also coauthored the textbook *Spheroidal Wave Functions in Electromagnetic Theory* (New York: Wiley, 2002). His current research interests are electromagnetic (EM) wave propagation and scattering, antenna design and analysis, and electromagnetic compatibility (EMC). He is an Editorial Board member of *Microwave and Optical Technology Letters* and *Wireless Personal Communications*.

Dr. Leong is a member of the Massachusetts Institute of Technology (MIT)-based Electromagnetics Academy and is a Fellow of the Institute of Electrical Engineers (IEE), U.K. He is the founding chairman of the Singapore IEEE Microwave Theory and Techniques Society (IEEE MTT-S)/IEEE Antennas and Propagation Society (IEEE AP-S) Chapter.